PROCEEDINGS, 47th Workshop on Geothermal Reservoir Engineering
Stanford University, Stanford, California, February 7-9, 2022
SGP-TR-223

Development of Downhole Measurement to Detect Inflow in Fractured Enhanced Geothermal Systems (EGS) Wells

Sarah Sausan, Luthfan Hafizha Judawisastra, Roland Horne

Dept. of Energy Resources Engineering, 367 Panama St., Stanford University, Stanford, CA, USA, 94305

sausan@stanford.edu, luthfan@stanford.edu, horne@stanford.edu

Keywords: chloride concentration, fracture inflows, EGS, Utah FORGE

ABSTRACT

The ability to measure inflow from fractures formed after a stimulation is crucial to assess the success of Enhanced Geothermal Systems (EGS) wells. A downhole technique was proposed to detect and quantify inflows from individual fractures by measuring the chloride ion concentration along the wellbore. The technique is being developed in preparation for a field test at the Utah Frontier Observatory for Research in Energy (FORGE) site.

Analytical calculations from a previous study were modified to suit the fractured EGS well configuration and expanded to consider the case of a well with multiple fracture zones. Measurement error stochastic modeling at a single feed zone (i.e., single fracture zone) shows that measurement error may adversely affect the accuracy of flow rate estimates at and below a feed zone, although less so above a feed zone.

Laboratory experiments were conducted to reconfirm tool calibration from the previous study and obtain data for measurement error. Calibration results were qualitatively in agreement with the previous study, and the accuracy of the calculated chloride concentrations showed a promising result. Further calibration trials are planned to improve the accuracy of the voltage-chloride relationship. Finally, data collected from the Geothermal Data Repository (GDR) and previous studies were analyzed to plan for the field test. The analysis points to well 58-32 as the most suitable candidate to test the ruggedized wireline version of the chloride measurement tool.

The ongoing work will further improve the analytical approach and laboratory experiments in preparation for the field test. In addition, the study will also perform numerical simulations using computational fluid dynamics to better understand the fluid mechanics of the fracture inflows within the wellbore.

1. INTRODUCTION

After a stimulation is performed in an EGS well, it is important to be able to confirm which fractures are flowing and at what rate. Gao, et al. (2017) developed a downhole tool to measure enthalpy in two-phase flow along a wellbore. The tool measures chloride concentration changes as an indirect way to estimate enthalpy. Because chloride always stay in the liquid phase, a change in chloride concentration reflects change in flowing steam fraction, which can be calculated back to the enthalpy of the liquid and steam phases.

This study expands Gao at al. (2017) approach to be applicable to EGS wells with single-phase flow, and has as its objective the location and quantification of fracture feed zones in the well. Ultimately, the approach will be field tested at the Utah FORGE site. The Utah FORGE site is located south of Salt Lake City and close to the Roosevelt Hot Springs. The site is a testing ground for scientific investigations in geothermal technology development, with four wells having more than 5000 ft MD depth. At Utah FORGE wells, the fluid is mostly in the liquid phase with little to no steam.

Four approaches are being conducted to produce optimum tool design and measuring techniques: analytical approach, laboratory experiment, numerical flow simulation, and field testing. This paper outlines the current progress of analytical approach and laboratory experiments, as well as initial planning for the field test.

2. METHODS

2.1 Analytical Approach

The analytical approach is based on Gao, et al. (2017) chloride mass balance principles. Some changes have been made to the original method to better suit the fractured EGS context, as follows:

- The original method was developed for multiphase flow. For this research, the method is modified to be applicable to for single-phase flow (i.e., in liquid state) in representation of conditions at the Utah FORGE field.
- Some terminology definitions are modified. For instance, single feed zone refers to a well with one fracture zone intersecting, whereas a well with multiple fracture zones is defined as having multiple feed zones.

- The symbol notations were changed for clarity and simplicity. Because the system is exclusively in liquid phase, the volumetric flow rate above the feed zone is notated with q_{above} instead of q_l, and the liquid indicator (l subscript) is dropped from all notations.

The modified analytical approach relies on the assumption that the chloride concentration and the volumetric flow rate at the wellhead ($Cl_{wellhead}$ and $q_{wellhead}$, respectively) can be obtained, and the chloride concentration at the feed zone (Cl_{in}), above the feed zone (Cl_{above}), and below the feed zone (Cl_{below}) can be measured by the downhole tool. Figure 1 illustrates the schematics of single feed zone wells vs. multiple feed zone wells and their calculation parameters.

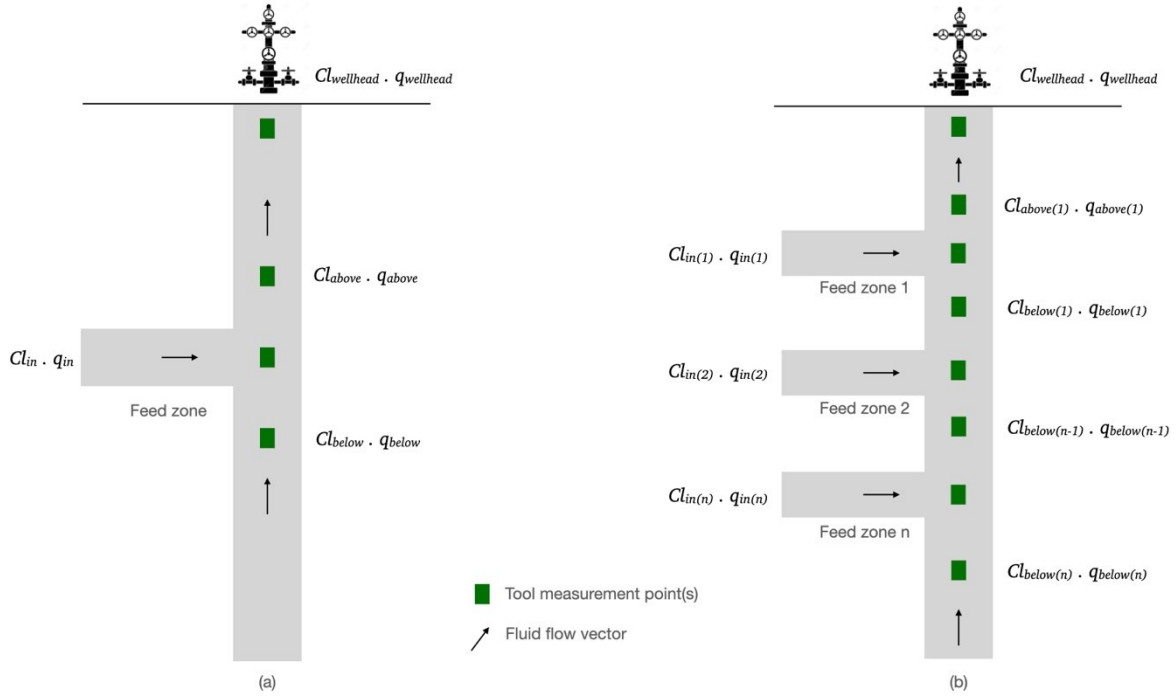

Figure 1: Schematics of a well with (a) single feed zone and (b) multiple feed zones. $Cl_{x(n)}$ represents the chloride concentration in kg/m^3 and q_x represents the volumetric flow rate in m^3/s. The subscript *x* denotes the measurement position, i.e., above feed zone (*above*), at feed zone (*in*), below feed zone (*below*), and at the wellhead (*wellhead*). The subscript *n* denotes the feed zone number for the multiple feed zones case.

2.1.1 Single feed zone

Gao, et al. (2017) describes that chloride mass balance principles can be applied to calculate liquid flow rate using concentrations measured at the positions indicated in Figure 1(a):

$$Cl_{in} \cdot q_{in} + Cl_{below} \cdot q_{below} = Cl_{above} \cdot q_{above} \quad (1)$$

$$q_{below} = q_{above} - q_{in} \quad (2)$$

Furthermore, chloride mass balance is maintained between the wellhead and above the feed zone, which is the basis for calculating flow rate above the feed zone:

$$q_{above} = \frac{Cl_{wellhead} \cdot q_{wellhead}}{Cl_{above}} \quad (3)$$

Using similar chloride mass balance principles, the flow rate at the feed zone can be derived from Equations (1) and (2):

$$\begin{aligned} Cl_{below}(q_{above} - q_{in}) + Cl_{in} \cdot q_{in} &= Cl_{above} \cdot q_{above} \\ Cl_{below} \cdot q_{above} - Cl_{below} \cdot q_{in} + Cl_{in} \cdot q_{in} &= Cl_{above} \cdot q_{above} \\ Cl_{in} \cdot q_{in} - Cl_{below} \cdot q_{in} &= Cl_{above} \cdot q_{above} - Cl_{below} \cdot q_{above} \\ (Cl_{in} - Cl_{below}) q_{in} &= (Cl_{above} - Cl_{below}) \cdot q_{above} \end{aligned}$$

The flow rate at the feed zone therefore can be calculated with the following formula:

$$q_{in} = q_{above}\frac{Cl_{above} - Cl_{below}}{Cl_{in} - Cl_{below}} \quad (4)$$

The fraction in Equation (**4**) can be written as Cl_{ratio} such that:

$$Cl_{ratio} = \frac{Cl_{above} - Cl_{below}}{Cl_{in} - Cl_{below}} \quad (5)$$

The flow rate below the feed zone can be calculated by using the similar chloride mass balance approach then inserted to Equation **Error! Reference source not found.**, such that:

$$q_{below} = q_{above} \cdot (1 - Cl_{ratio}) \quad (6)$$

2.1.2 Multiple feed zones

As illustrated in Figure 1, we expanded the single feed zone calculation to account for more than one feed zones. Denoting the topmost feed zone as feed zone 1, followed by feed zone 2, *ad infinitum* such that feed zone can be denoted with *n*. The flow rate calculations for feed zone 1 are the same as with single feed zone calculations. The volumetric flow rate calculations for feed zone *n* where $n > 1$ are:

$$Cl_{ratio(n)} = \frac{Cl_{below(n-1)} - Cl_{below(n)}}{Cl_{in(n)} - Cl_{below(n)}} \quad (7)$$

$$q_{above(n)} = q_{below(n-1)} \quad (8)$$

$$q_{in(n)} = q_{below(n-1)} \cdot Cl_{ratio(n)} \quad (9)$$

$$q_{below(n)} = q_{below(n-1)} \cdot (1 - Cl_{ratio(n)}) \quad (10)$$

2.1.3 Error Estimation

Gao (2017) did a series of experiments to determine the average relative error of measured chloride concentration versus actual known chloride concentration with respect to different gas flow rates. It was found that for liquid flow, the measurement underestimated the actual chloride concentration by around 1.2%. However, the noise level at the feed zone could be different than at the well head or above or below the feed zone. Therefore, relative error of chloride measurement at various points at the wellbore and its effect to the resulting flow rate calculations need to be understood.

The average relative error of the chloride measurement can be represented with error factor e_f, which upon multiplying with the measured value, will give the corrected chloride measurement, such that:

$$Cl_{corr} = Cl_{measured} \cdot e_f \quad (11)$$

where Cl_{corr}, $Cl_{measured}$, and e_f are corrected chloride measurement, measured chloride measurement, and average relative error factor, respectively. The chloride ratio in Equation (5) can then be corrected accordingly to account for relative error fluctuating at different points in the wellbore:

$$Cl_{ratio(corr)} = \frac{Cl_{above} \cdot e_{fabove} - Cl_{below} \cdot e_{fbelow}}{Cl_{in} \cdot e_{fin} - Cl_{below} \cdot e_{fbelow}} \quad (12)$$

The volumetric flow rate calculations for both single feed zone and multiple feed zones can be corrected in a similar manner, where each of the measured flow rate concentration is multiplied by its error factor.

2.1.4 Error Modeling

Taking the formulas defined in Section 2.1.1, the range of discrepancies between uncorrected and corrected chloride measurements at various points of the wellbore were modelled stochastically to understand their effect on the resulting flow rate calculations. Numerical simulations involving 1000 runs of flow rate calculations were performed with randomly distributed *e* values, using rectangular and normal distribution methods for comparison.

Figure 2 shows a snapshot of the *e* value distribution for each type of random distribution and the resulting mass flow rate calculations in a well with single feed zone. As expected, the simulation results show that normally distributed error value yields narrower volumetric flow rate range compared to rectangular distribution. The range of q_{above} is consistently narrower than q_{in} and q_{below} with the latter pair being similar in range to each other.

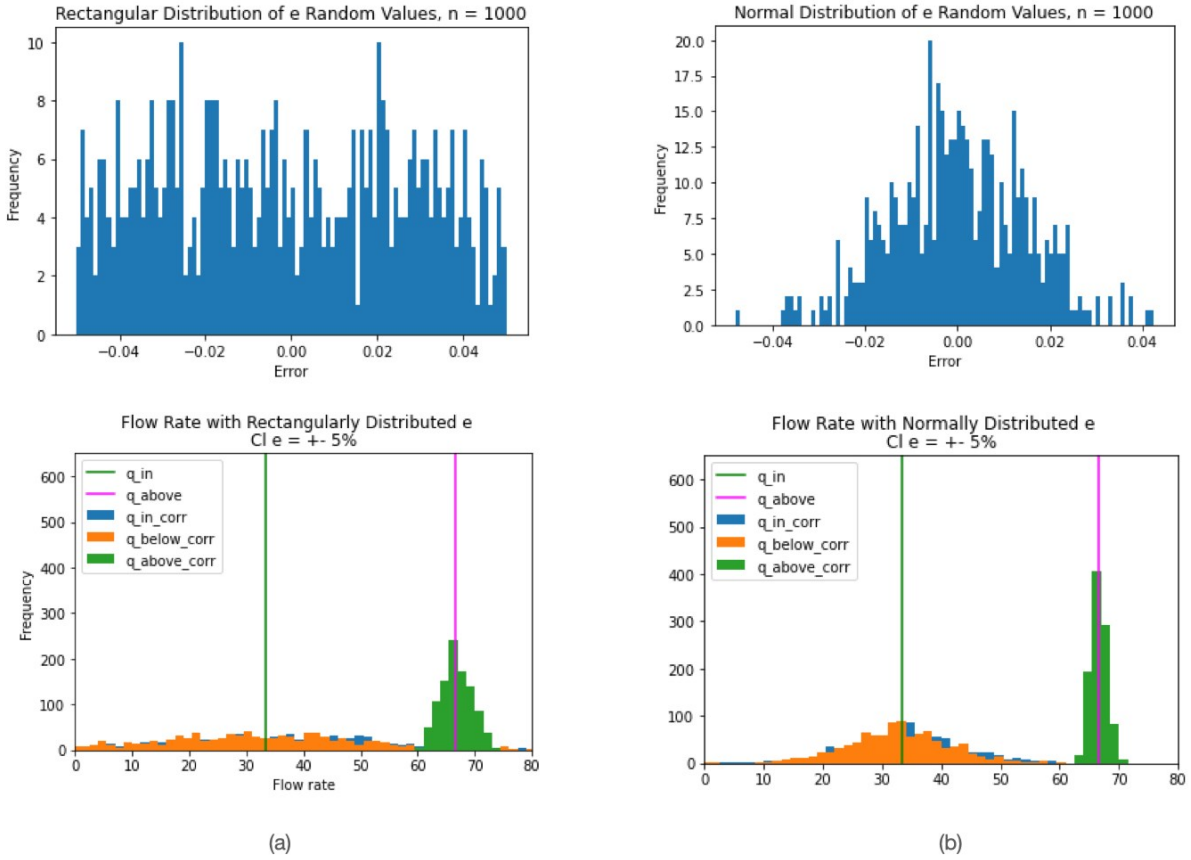

Figure 2: Snapshots of *e* distribution and resulting volumetric flow rate calculation for a well with single feed zone with (a) rectangular and (b) normal distribution methods.

For each distribution, different error ranges were tested, namely ± 1.5%, ± 3%, and ± 5%, all with 500 intervals (Figure 3). There is a positive correlation between increasing error ranges and increasing the flow rate ranges, and q_{above} consistently have narrower range compared to q_{in} and q_{below} with the latter pair being similar in range to each other.

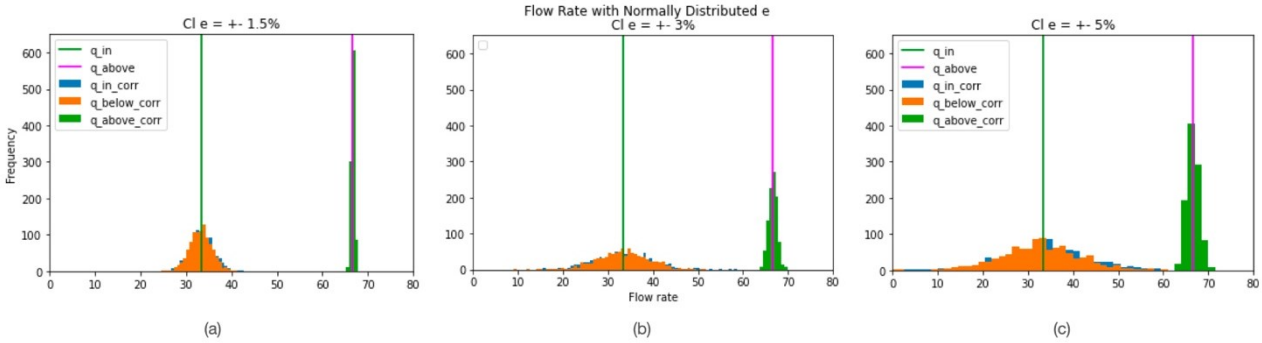

Figure 3: The simulation result of resulting volumetric flow rate calculations for the different ranges of *e*: (a) ± 1.5%, (b) ± 3%, and (c) ± 5%.

From the error modeling for single feed zone case, it can be concluded that measurement error will adversely affect the accuracy of volumetric flow rate calculations at and below the feed zone, but not so much above the feed zone.

2.2 Laboratory Experiments

Laboratory experiments were conducted using the same Sandia prototype chloride measurement tool as used by Gao, et al. (2017). The downhole tool was developed by Sandia National Laboratories and has the dimension of 29.3 cm in length and 2.65 cm in diameter. The tool consists of three electrodes: a chloride-ion selective electrode (Cl-ISE), a solid-state bimodal pellet reference electrode and a graphite

ground reference electrode. Details of the tool assembly and operational procedures were described by Cieslewski et al. (2016), Corbin et al. (2017), and Gao, et al., (2017). A diagram of the assembled tool is shown in Figure 4.

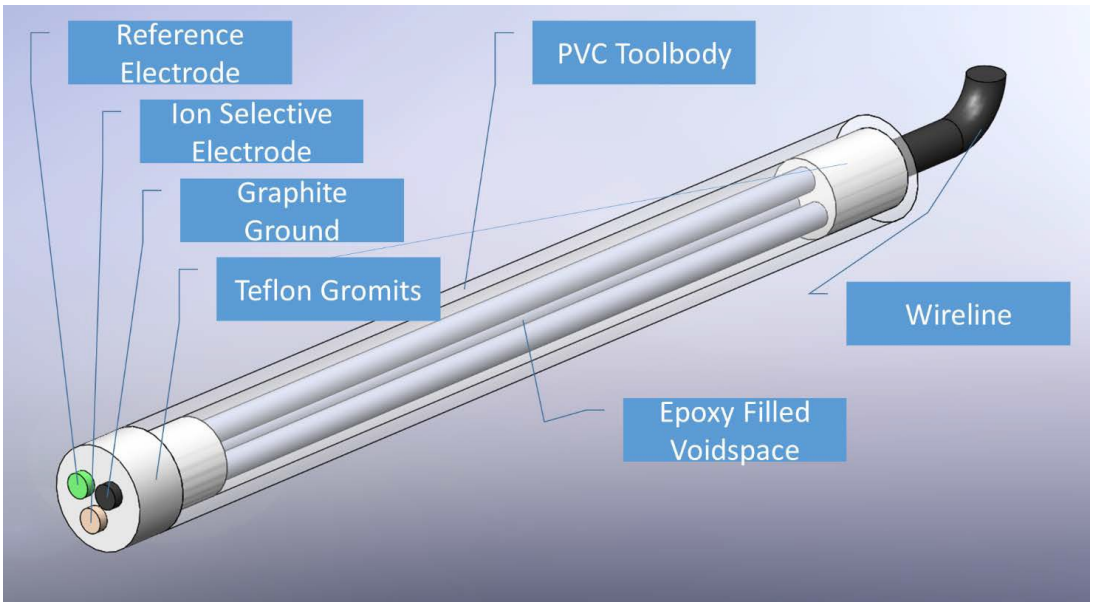

Figure 4: cut-away diagram of the benchtop version of the tool used in this study (Gao et al., 2017)

2.2.1 Tool Calibration

The tool was calibrated to obtain an updated relationship between voltage reading and chloride concentration. Voltage was measured in gradually increasing concentrations of sodium chloride dissolved in water at ambient condition. The tool was fully submerged during the measurement takes with a multimeter attached at the electrodes, as shown in in Figure 5.

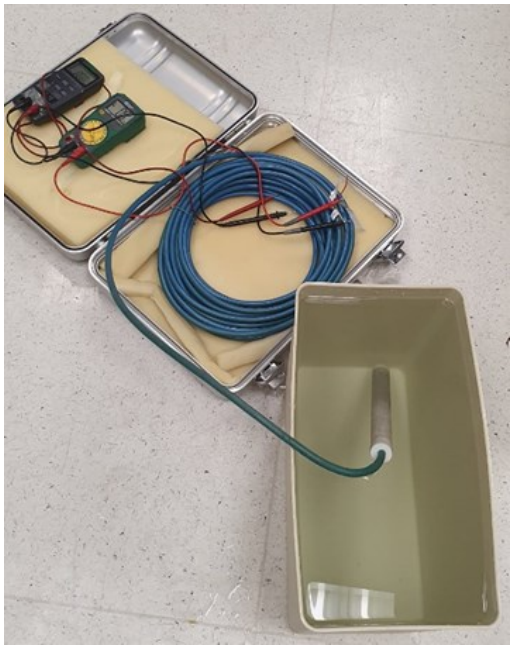

Figure 5: Tool calibration setup

As many as 15 calibration data points were obtained, ranging from a chloride concentration of 10^{-6} mol/L up to 1 mol/L (Figure 6). Compared with the calibrations results of Gao (2017), the updated calibration shows a smaller voltage reading for the same concentration of chloride. However, the trendline is still similar, with higher salt concentration resulting in smaller voltage readings.

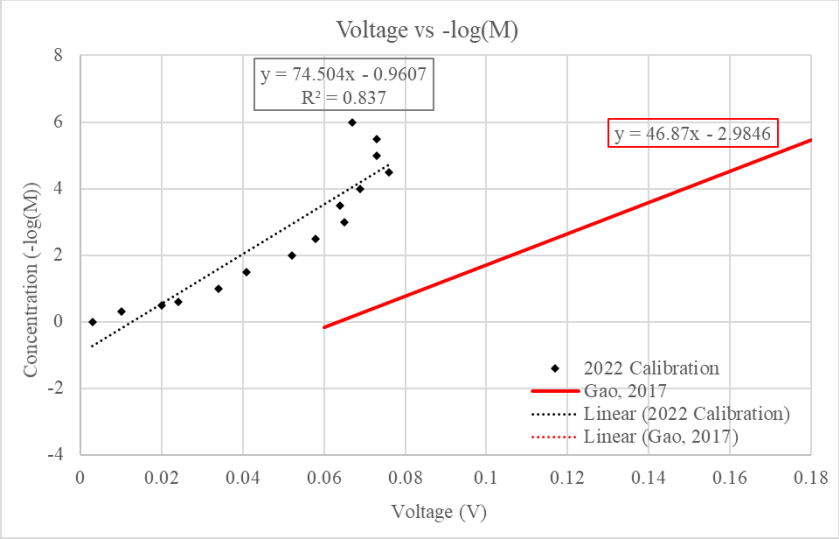

Figure 6: Tool calibration result

The relationship between voltage readings and chloride concentrations of the updated calibration is shown in Equation (13) with regression coefficient (R^2) of 0.837, with M being chloride concentration in mol/L and V being the voltage in volts.

$$-\log(M) = 74.50V - 0.96 \tag{13}$$

Calibration conducted by Gao (2017) shows a higher regression coefficient (0.99) which is shown by Equation (14):

$$-\log(M) = 48.67V - 2.9846 \tag{14}$$

Therefore, further improvement of the calibration procedure needs to be done in order to get a closer relationship between voltage reading and chloride concentration. It is also necessary for us to examine whether the tool performance has degraded over the five years since the previous calibration was made.

2.2.2 Artificial Well System

The laboratory experiments used an artificial well system to represent flow in a vertical well with feed zones. The well system consists of a main wellbore with 5.5-inch diameter and 71.3-inch height, a reservoir tank of around 200 L in capacity located at the bottom of the well, and three feed zone ports (Figure 7). During the experiment runs, water from the reservoir tank was pumped from the reservoir tank into the bottom of the well, which then flowing to the top of the well until being circulated back to the reservoir tank by the circulation pipes. The feed zone ports at the side of the wells can be used to inject fluids into the main wellbore. The first, second and third feed zone ports are 34, 50 and 60 inches apart from the bottom of the well, respectively. The second feed zone port is on the opposite side of the first and third feed zone port.

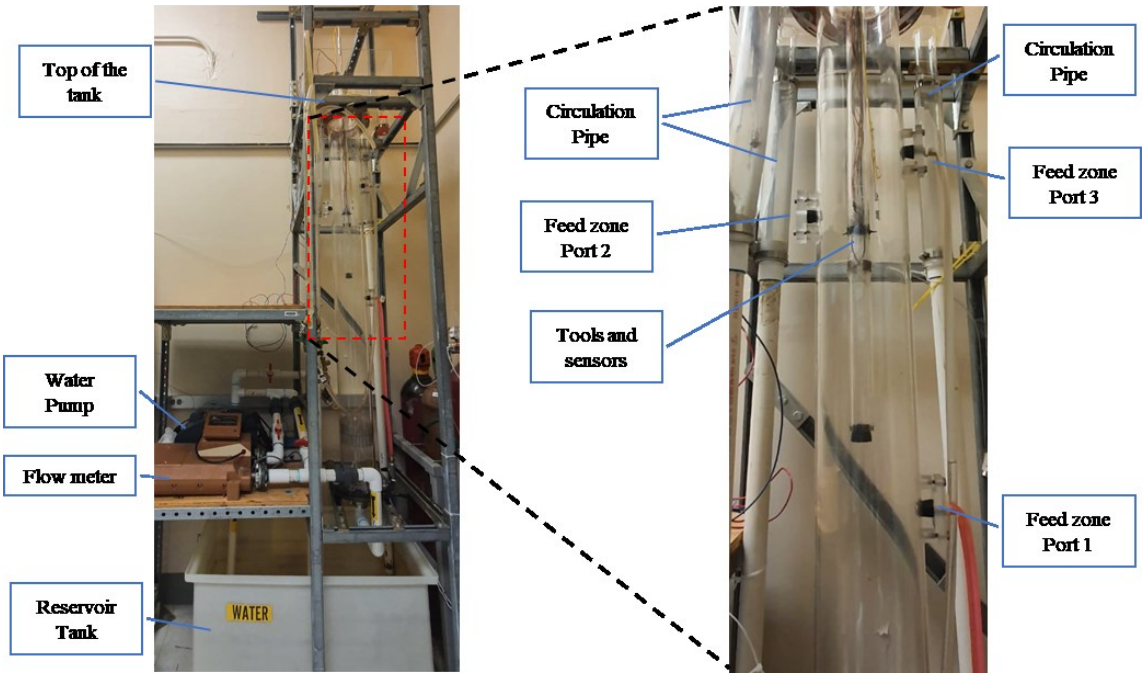

Figure 7: Artificial well system

2.2.3 Downhole Flow Chloride Measurement

Apart from the tool calibrations, a laboratory experiment to test the chloride measurement in bulk vs. inside the wellbore was conducted. A single-phase flow with different chloride concentrations was conducted with water containing chloride concentrations ranging from 0.5 mol/L to 0.0625 mol/L. Voltage were measured both in the reservoir tank and inside the well while the water was circulating. The measurement inside the well was obtained by attaching the tool with a 36-inch metal rod and inserting the rod into the well from the top. A comparison between the voltage readings from the reservoir tank and inside the well is shown in Figure 8. While the voltage measurements at wellbore shows a slightly higher reading, generally there is no significant difference between well and reservoir voltage readings.

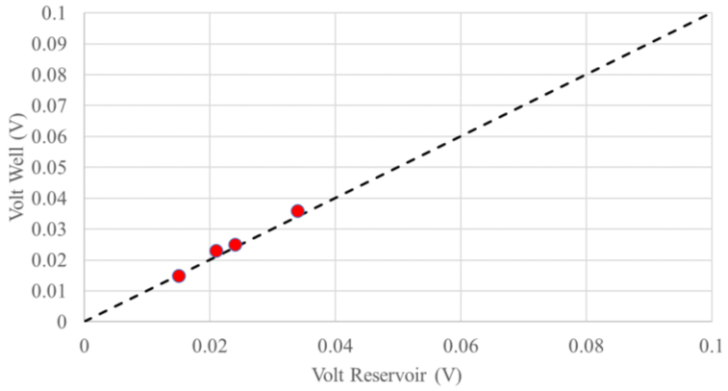

Figure 8: Well and reservoir tank voltage readings

Voltage measurement was then converted to chloride concentration by using Equation (13). Figure 9 shows the calculated chloride concentrations from the voltage readings obtained at the well and the reservoir tank compared to the actual known concentration. The actual concentration was obtained by diluting a 0.5 mol/L solution with water to double the volume, resulting in half the concentration. The procedure was repeated until reaching the data point with the least concentration. The result shows a relatively good match between the actual concentrations and the calculated concentrations for concentration lower than 0.3 mol/L. However, chloride concentration higher than 0.3 mol/L only has one data point at 0.7 mol/L calculated concentration vs. 0.5 mol/L actual concentration. This is a variance of the voltage-chloride relationship from Equation (13) as the regression is less than the previous study. From this run, it was learned that: 1) improving the calibration techniques will positively affect the calculated concentrations, and 2) more data points are needed to generate a more comprehensive relationship.

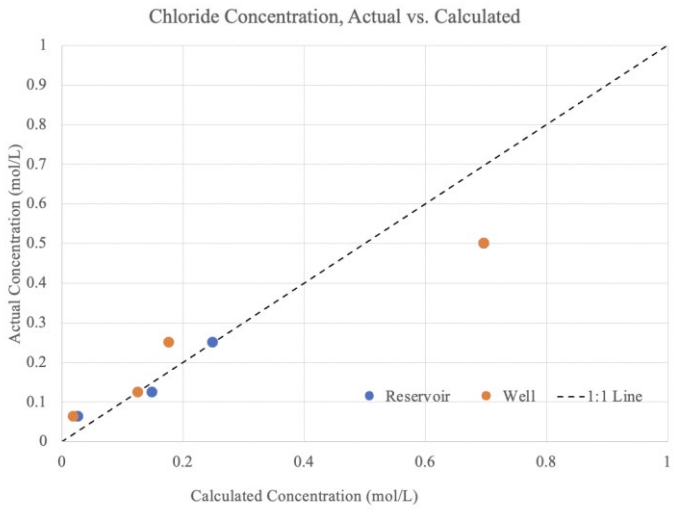

Figure 9: Concentration actual vs. calculated concentration from voltage

After improving the calibration techniques and getting a satisfactory result, the laboratory experiments will continue to test chloride measurements with different cases of chloride concentration and the number of active feed zones.

3. FIELD TESTING PLAN

A field test is planned in Utah FORGE site using a ruggedized wireline version of the chloride measurement tool. The existing and planned wells were evaluated to determine suitability and feasibility to be the primary candidate for running the chloride measurement tool (Figure 10). There are currently four existing wells at the site: 16A(78)-32 (injection well), 58-32 (pilot well), 78B-32, and 56-32 (both are seismic monitoring wells). Additionally, two wells are planned to be drilled in 2022: 16B(78)-32 (production well) and Well 47-32 (seismic monitoring well).

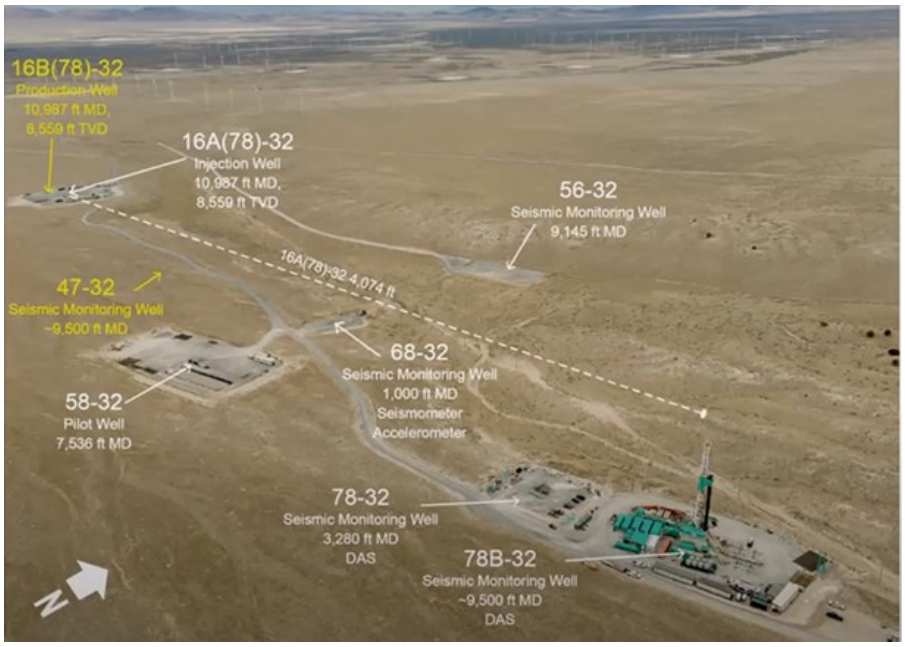

Figure 10: Utah FORGE wells (Xing, et al., Utah FORGE modelling and simulation forum, 15th Sep 2021) showing existing wells (labeled in white) and planned wells (labeled in yellow).

Figure 11 illustrates the temperature measurements taken in the Utah FORGE wells between 2017 and 2021. Temperature for 78B-32 (shown as red star) was extrapolated from the temperature trend, while data 78B-32 (shown as black star) was measured directly after pumping during drilling. The highest measured temperature of the reservoir was 433^{0}F at depth around 9000 ft MD. The data shows that the thermal gradient is relatively homogeneous across the Utah FORGE wells, meaning that temperature is not considered as a factor in determining the well candidate.

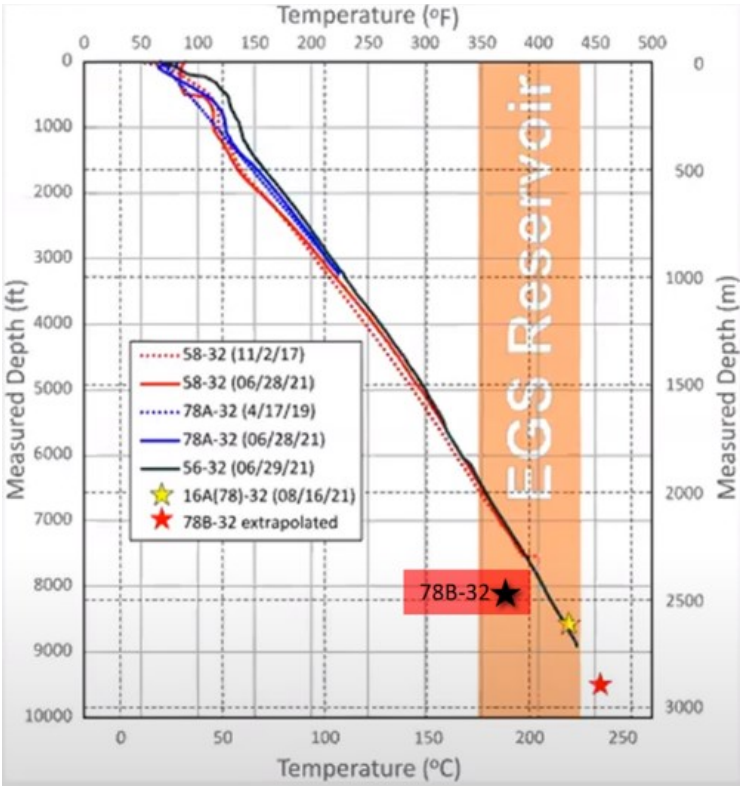

Figure 11: Utah FORGE field wells temperature measurements (Edited from Xing, et al., Utah FORGE modelling and simulation forum, 15th Sep 2021).

Using the available data in Geothermal Data Repository (GDR), the four existing wells were compared to determine which would be the most suitable candidate for the field test of the chloride tool (Table 1). To obtain representative data for the field, it is favorable to work with deeper wells. While 16A(78)-32 is the longest well by MD and the only directional well in the site (currently), 56-32 is the deepest by TVD (9145 ft TVD). Furthermore, to obtain chloride measurement data that are representative of the reservoir, the well candidates must have good conduits between the inside of the wellbore and the reservoir. The GDR data showed that 58-32 was stimulated at three different depths in 2017-2019, 16A(78)-32 was stimulated once at the bottom of the well in 2021, while 56-32 and 78B-32 were not stimulated. Considering the homogeneous thermal gradient across the field and the number of stimulation that each well have, 58-32 seems to be the best candidate to conduct the chloride measurement test.

Table 1: Comparison of Utah FORGE Wells (Geothermal Data Repository, 2022)

	58-32	16A(78)-32	56-32	78B-32
Casing Shoe	13-3/8" @ 337 ft MD 9-5/8" @ 2173 ft MD 7" @7378 ft MD	13-3/8" @ 1629 ft MD 9-5/8" @ 5110 ft MD 7" @10787 ft MD	13-3/8" @ 382 ft MD 9-5/8" @ 3494 ft MD 5-1/2" @9105 ft MD	13-3/8" @ 416 ft MD 9-5/8" @ 2990 ft MD 7" @8509 ft MD 5-3/4 Hole to 9500 ft
Well Inclination	No	Yes	No	No
Max. Temp (°F)	385° F Taken 06/28/2021	425° F Interpolated from Utah FORGE modelling and simulation forum, 2021	433° F Taken 06/29/2021	353.7° F @ 8540 ft Taken 07/19/2021, 10.625" and 8.75" Open hole, during drilling (post pumping)

Feed Zone Indication	**6565-6575 ft** MD (perforated casing, stimulated 2019) **6964-6975 ft MD** (perforated casing, stimulated in 2019) **7375-7525 ft** MD (Barefoot, Stimulated in 2017)	**10787-10987** ft MD (Barefoot, 2021) Stimulation planned for Q2 2022 and Q3 2023 Flow testing planned for Q3 2022 and 2024		

Well 58-32 is a vertical well that was drilled in 2017 to a total depth of 2297 m (7536 ft). The well has two perforation intervals with a 150-m open hole section at the bottom (see Table 1). The well was projected to penetrate the reservoir at around 6500 ft. After the well was completed, FMI logging, sonic logging, and other geophysical survey methods were run. Additionally, two cores approximately 22 ft long were obtained, followed by one stimulation job at the open hole section. In 2019, three stimulation jobs were performed: one at each of the two perforation intervals and one at the bottom hole. The latest downhole temperature measurement was taken in June 2021 up to 7510 ft MD and with the highest temperature at 385° F. Figure 12 shows the summary of activities that have been conducted at well 58-32 between 2017 and 2019.

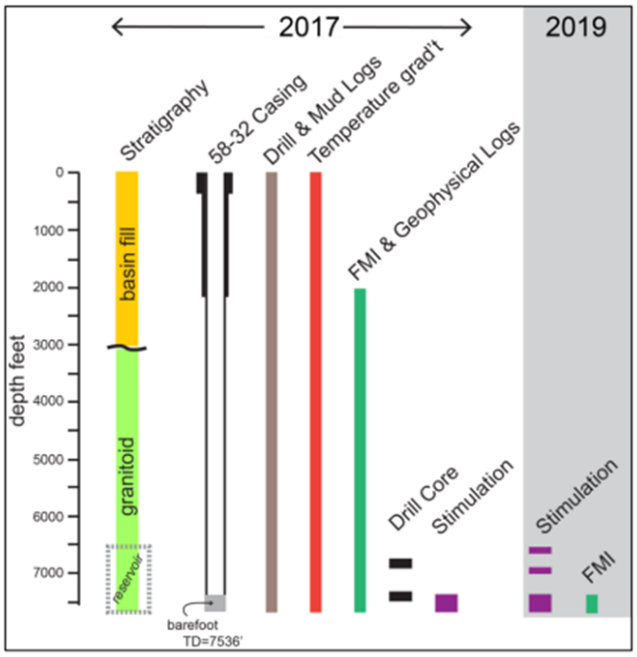

Figure 12: Summary of major activities conducted in well 58-32 in 2017 and 2019. (Moore, et al., 2020)

Considering that the laboratory experiments use a vertical well setup, running the field test at 58-32 will be comparable. A vertical well will also have fewer challenges during a wireline survey compared to a directional well. To ensure accuracy of the obtained data and the operation success, it is recommended that any other tool installed within the wellbore is removed prior to running the chloride measurement tool.

4. CONCLUSION

Expanding the work of Gao, et al. (2017) to a flow monitoring application at Utah FORGE introduces additional complexity to the analytical approach and laboratory experiments, especially because the best well candidate (58-32) has multiple feed zones. The stochastic modeling of measurement error for single feed zone (i.e., single fracture zone) case shows that measurement error may affect the accuracy of flow rate at and below a feed zone, although less so above a feed zone. It is predicted that in the field test, the measurement error will especially affect the intervals that are close to each other. Thus, one of the early objectives of the laboratory experiments and the upcoming numerical simulations is to determine the effective resolution of the measurement tool in terms of the smallest fracture zones separation that it can differentiate.

ACKNOWLEDGEMENT

This work forms part of the Utah FORGE project and is being conducted in collaboration with Sandia National Laboratory and supported by the U.S. Department of Energy.

REFERENCES

Cieslewski, G., Hess, R. F., Boyle, T. J., Yelton, W. G.: Development of a Wireline Tool Containing an Electrochemical Sensor for Real-time pH and Tracer Concentration Measurement, GRC Transactions, Vol.40, (2016).

Corbin, W. C., Cieslewski G., Hess R. F., Klamm B. E., Goldfarb L., Boyle T. J., and Yelton W. G.: Development of a Downhole Tool for Measuring Enthalpy in Geothermal Reservoirs, 42th Workshop on Geothermal Reservoir Engineering, Stanford University, Stanford, CA (2017).

Di Drill Survey Services. (2021). Utah FORGE Wells Updated Temperature and Pressure Logs (June 2021) [data set]. Retrieved from https://dx.doi.org/10.15121/1812334.

Gao, X.: Development of a Downhole Technique for Measuring Enthalpy in Geothermal Wells, Master Thesis, Department of Energy Resources engineering, Stanford University, Stanford, CA (2017).

Gao, X., Egan, S., Corbin, W.C., Hess, R.F., Cieslewski, G., Cashion, A.T., and Horne, R.N.: Analytical and Experimental Study of Measuring Enthalpy in Geothermal Reservoirs with a Downhole Tool, GRC Transactions, Vol.41, (2017).

Moore, J., McLennan, J., Pankow, K., Simmons, S., Podgorney, R., Wannamaker, P., Jones, C., Rickard, W., and Xing, P.: The Utah Frontier Observatory for Research in Geothermal Energy (FORGE): A Laboratory for Characterizing, Creating and Sustaining Enhanced Geothermal Systems, Proceedings, 45th Workshop on Geothermal Reservoir Engineering, Stanford University, Stanford, CA (2020).

Xing, P., Damjanac, B., Mclennon, J., Radakovic-Guzina, Z., Finnila, A., Podgorney, R., and Moore, J. "Pressure History Matching and Model Calibration" *Modelling and Simulation Forum*, Utah FORGE U.S. department of Energy, 15 September 2021, https://utahforge.com/2021/09/02/modeling-and-simulation-forum-10-recording/